

# Instruction-Grounded Visual Projectors for Continual Learning of Generative Vision-Language Models

Hyundong Jin<sup>1</sup>Hyung Jin Chang<sup>2</sup>Eunwoo Kim<sup>1,\*</sup><sup>1</sup>School of Computer Science and Engineering, Chung-Ang University<sup>2</sup>School of Computer Science, University of Birmingham

{jude0316, eunwoo}@cau.ac.kr

h.j.chang@bham.ac.uk

## Abstract

Continual learning enables pre-trained generative vision-language models (VLMs) to incorporate knowledge from new tasks without retraining data from previous ones. Recent methods update a visual projector to translate visual information for new tasks, connecting pre-trained vision encoders with large language models. However, such adjustments may cause the models to prioritize visual inputs over language instructions, particularly learning tasks with repetitive types of textual instructions. To address the neglect of language instructions, we propose a novel framework that grounds the translation of visual information on instructions for language models. We introduce a mixture of visual projectors, each serving as a specialized visual-to-language translation expert based on the given instruction context to adapt to new tasks. To avoid using experts for irrelevant instruction contexts, we propose an expert recommendation strategy that reuses experts for tasks similar to those previously learned. Additionally, we introduce expert pruning to alleviate interference from the use of experts that cumulatively activated in previous tasks. Extensive experiments on diverse vision-language tasks demonstrate that our method outperforms existing continual learning approaches by generating instruction-following responses.

## 1. Introduction

Generative Vision-Language Models (VLMs) [4, 33, 35, 55] have demonstrated remarkable performance in a variety of tasks, such as caption generation [24], visual question answering [42], and creative applications [1, 55]. Their impressive performance is attributable to the robust capabilities of large language models in conjunction with a translation module that enables these models to comprehend visual information from a visual encoder. Despite their remarkable performance, generative VLMs face significant

\*Corresponding author.

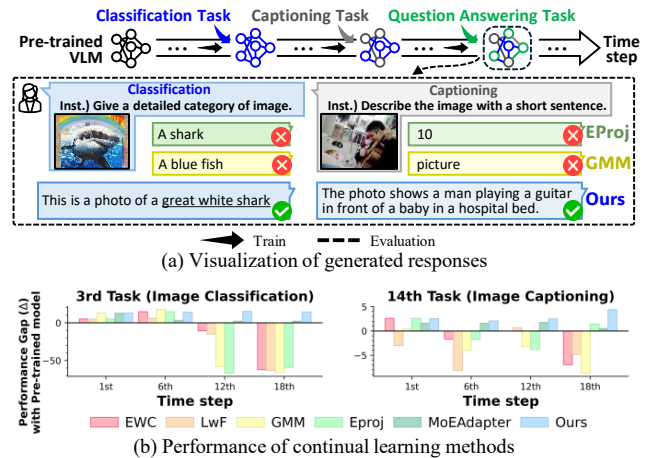


Figure 1. (a) Generated responses for classification and captioning tasks from continual learning methods for VLM after training on a question answering task. Existing methods, EProj [16] and GMM [4], neglect text instruction. (b) Performance gap between the pre-trained model and models trained on sequential tasks using various continual learning methods. The proposed method outperforms others in preventing knowledge forgetting.

challenges in adapting to newly emerging tasks. Retraining these models with pre-trained and newly acquired data imposes considerable computational costs due to the large volume of pre-trained data [26] and its limited public accessibility [40]. Furthermore, training models solely on new tasks leads to overwriting previously acquired knowledge, resulting in catastrophic forgetting [25, 37].

Continual learning methods [22, 23, 25, 31, 41, 48] aim to address these challenges by allowing models to incorporate new tasks while preserving old knowledge with access only to the data of newly emerging tasks. Existing continual learning methods rely on storing a small set of previous data and training it jointly with the new data [13, 41] or on regularizing parameter updates that are important for previous tasks [25]. Other methods [31, 44, 48] incorporate a small set of learnable parameters into pre-trained knowl-

edge to capture task-specific knowledge. Despite these advancements, continual learning for VLMs remains under-explored. Recently, a few studies [4, 52] proposed to directly update the pre-trained visual projector of VLM that converts visual features for language models to learn new tasks, where tasks share similar instruction templates accompanied by similar answer types. Although these methods show promising results for such tasks, they neglect text instructions for response generation after training on tasks with varying instructions, as shown in Figure 1 (a).

In this paper, we propose a novel framework for transforming visual information grounded on language instructions for continual learning of VLMs. To this end, we introduce a **Mixture of Visual Projectors**, named **MVP**, each serving as an expert dedicated to transforming visual information based on a given instruction context. In particular, our routing scheme dynamically adapts to both the semantic content of the instruction and the visual information, leveraging translation experts that align with the linguistic intent. To encourage the use of appropriate experts for given instructions, we propose an expert recommendation strategy that promotes reusing experts associated with relevant previous tasks while discouraging those specialized in other instructions. In addition, we propose expert pruning to mitigate negative transfer to future tasks induced by the reuse of redundantly activated experts in previous tasks. To preserve the zero-shot capabilities of pre-trained VLMs, we adaptively aggregate the transformed visual information from the proposed mixture of visual projectors and the pre-trained projector, calibrating their contributions based on the relevance of the given input data to the learned tasks.

To evaluate the proposed method, we perform vision-language tasks, including classification [17], captioning [39], and question answering [42], with a diverse range of visual and textual data. We evaluated its ability to retain new knowledge and maintain zero-shot performance, as illustrated in Figure 1 (b). The experimental results show that the proposed method outperforms its competitors by translating visual information for a given instructional context. The contributions of our work are four-fold:

- We propose a novel framework for adaptively translating visual information grounded in textual instruction for continual learning of generative vision-language models.
- We present expert recommendation and pruning strategies for sparse activation of experts from semantically relevant old tasks while mitigating negative knowledge transfer.
- To preserve zero-shot capabilities, we adaptively aggregate knowledge by balancing pre-trained and instruction context-aware projections.
- Extensive experiments show that the proposed framework outperforms other continual learning methods in preserving both pre-trained and newly learned knowledge.

## 2. Related Work

**Generative Vision-Language Models (VLMs)** [11, 29, 32, 49, 55] demonstrate notable zero-shot generalization and in-context learning capabilities for vision-language tasks. These models harness the robust capabilities of Large Language Models (LLMs) [9, 46] by employing connection modules that bridge the visual encoder with the LLM, e.g., Qformers [11, 29] or resampler [32, 49, 55]. By translating visual information into comprehensible representations for the language model, VLMs can interpret and generate responses based on complex visual and textual inputs. Updating the connection module can directly improve the visual information for the language model with negligible parameter updates compared to updating the visual encoder and the language model [5, 55]. However, this approach is vulnerable in that previously acquired information can be significantly compromised during adaptation to new vision-language tasks. Therefore, a central challenge in VLMs is preserving the ability to follow previously learned instructions while adapting to newly introduced ones.

**Continual Learning** aims to learn from a stream of tasks without forgetting previously acquired knowledge [25, 37]. Existing continual learning methods incorporate additional regularization terms to penalize changes in critical parameters to maintain performance on earlier tasks [3, 6, 25, 51], or replay a memory buffer containing a small set of data from previous tasks when learning new tasks [13, 34, 41]. Continual learning with parameter-efficient tuning methods [15, 44, 47, 48] learns task-specific representations by selectively updating a minimal subset of parameters [19, 21]. Recently, several approaches for continual learning in visual language models [4, 52] incorporate a visual projector that is shared across tasks. Although these approaches might be beneficial for tasks that share similar instruction templates, learning tasks that include contextually different instructions might cause the model to easily forget the previously learned visual representations. In contrast, the proposed approach addresses this limitation by leveraging context-aware visual-to-language translation for given textual instructions.

**Mixture-of-Experts (MoE)** [8, 20, 36, 38, 50] consists of multiple distinct networks, called experts, and a routing network to select appropriate experts and aggregate the outputs of the selected experts. In continual learning, MoE-based methods have been introduced [2, 8, 50] by expanding the router [2, 8, 50] or adding more experts [2, 8] in response to new tasks. Additionally, existing methods [8, 50] prohibit updates to a subset of experts associated with old tasks to mitigate forgetting when learning new tasks. However, this can potentially hinder learning for new tasks by freezing important experts, and a large number of frozen experts complicates capturing new representations. In this work, we resolve these limitations by recommending experts to

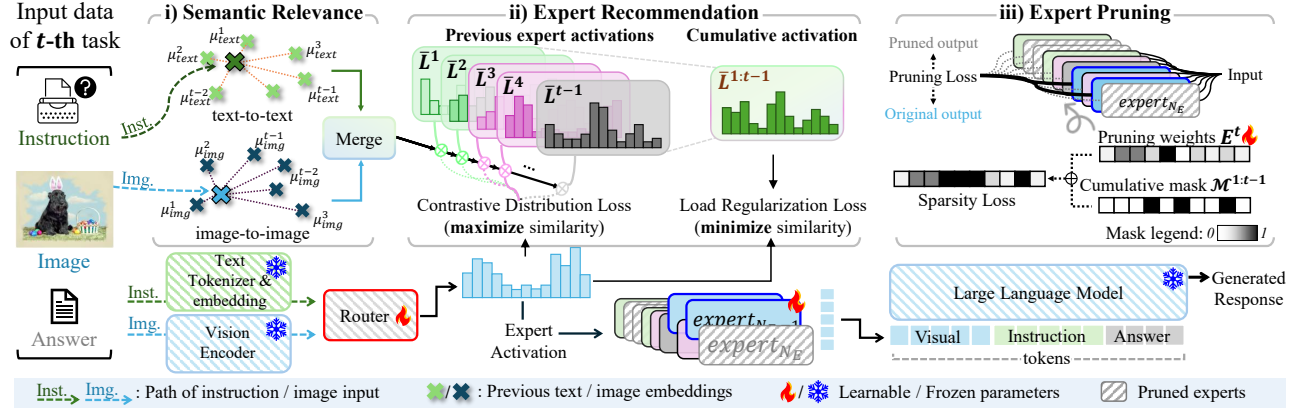


Figure 2. An illustration of the proposed continual learning framework for the  $t$ -th vision-language task. A router determines projector (expert) activations based on the embeddings of the instruction and image. To prevent detrimental expert activation of a router, (i) we first evaluate the semantic relevance between the current and previous tasks within an embedding space. (ii) We then encourage the activation of experts used in semantically related previous tasks for new tasks, while suppressing those with high cumulative activation frequencies. (iii) To mitigate negative knowledge transfer to subsequent tasks, we prune and reinitialize experts with parameters of the pre-trained projector, thus securing learning capacity for subsequent tasks. Finally, the large language model generates responses through vision, instruction, and answer tokens.

be updated based on their relevance to the new task while preventing reliance on irrelevant ones, ensuring that experts remain active to provide sufficient learning capacity for new tasks. In addition, we propose expert pruning to break the cycle of negative knowledge transfer caused by regularizing balanced expert utilization, which risks subsequent tasks reusing redundantly updated experts from previous tasks.

### 3. Methodology

#### 3.1. Overview

Continual learning aims to enable pre-trained generative vision-language models (VLMs) to preserve previously acquired knowledge while sequentially adapting to a sequence of novel tasks. At time step  $t$ , VLM is trained on the  $t$ -th vision-language task, where the  $t$ -th task  $T^t = \{x_i^t, q_i^t, y_i^t\}_{i=1}^{N^t}$  comprises  $N^t$  triplets, where  $x_i^t$ ,  $q_i^t$ , and  $y_i^t$  represent an image, a text instruction, and a text-based answer for the  $i$ -th sample, respectively. For each triplet, the image feature  $\mathbf{x}_{i,\text{img}}^t = \mathcal{F}_v(x_i^t)$  is extracted by the vision encoder  $\mathcal{F}_v$ , and the instruction tokens  $\mathbf{x}_{i,\text{text}}^t = \mathcal{F}_e(q_i^t)$  and the answer tokens  $\mathbf{y}_i^t = \mathcal{F}_e(y_i^t)$  are extracted by the text embedding function  $\mathcal{F}_e$  of the pre-trained model.

To make the image feature  $\mathbf{x}_{i,\text{img}}^t$  compatible with the language model, a visual projector  $\mathcal{V}$  transforms it into  $\tilde{\mathbf{x}}_{i,\text{img}}^t = \mathcal{V}(\mathbf{x}_{i,\text{img}}^t)$ . Then the auto-regressive decoder  $\mathcal{D}$  generates responses by receiving the tokens  $\tilde{\mathbf{x}}_{i,\text{img}}^t$ ,  $\mathbf{x}_{i,\text{text}}^t$ , and  $\mathbf{y}_i^t$ . A naïve method to learn a new task is to update the pre-trained visual projector to align the predicted responses with the answer tokens by minimizing the cross-entropy loss as  $\mathcal{L}_{ce} = -\sum_{i=1}^{N^t} \sum_{j=1}^L \mathbf{y}_{i,j}^t \log \hat{\mathbf{y}}_{i,j}^t$ , where  $L$

denotes the number of tokens in the response.  $\mathbf{y}_{i,j}^t$  denotes the  $j$ -th token of the answer for the  $i$ -th sample, and  $\hat{\mathbf{y}}_{i,j}^t$  denotes the corresponding predicted token.

Although updating the visual projector of a VLM is a parameter-efficient approach [4, 16], training it with similar repetitive instructions restricts its translation ability to reflecting only those instruction contexts. This results in the model neglecting different text instructions, as illustrated in Figure 1 (a). To address this, we propose a novel framework that adaptively translates visual information via a mixture of projectors to provide instruction-context aware visual translation. To encourage the use of projectors for relevant contexts, we introduce a recommendation strategy that promotes the activation of projectors associated with semantically similar previous tasks. Additionally, we present expert pruning to eliminate redundant experts that may cause negative transfer to subsequent tasks. The overall framework is illustrated in Figure 2.

#### 3.2. Mixture-of-Visual Projectors

We present a method to adaptively adjust visual projectors grounded on the text instructions of a new task. Our framework includes a router  $\mathcal{R}$  and a set of projectors (experts)  $\{\mathcal{E}_j\}_{j=1}^{N_E}$ , each contributing as a visual-to-language translator for the given instructional context. For the  $t$ -th task, the router takes in multimodal data  $\mathbf{x}_{i,\text{img}}^t$  and  $\mathbf{x}_{i,\text{text}}^t$  to select the appropriate experts for translating  $\mathbf{x}_{i,\text{img}}^t$  for a language model. The aggregated output from the selected experts is

$$\tilde{\mathbf{x}}_{i,\text{img}}^t = \sum_{j=1}^{N_E} w_j \mathcal{E}_j(\mathbf{x}_{i,\text{img}}^t), \quad (1)$$

where  $w_j$  denotes the routing weight determined by  $\mathcal{R}$ , which quantifies the contribution of the  $j$ -th expert. To ensure the visual projector grounded on the text instructions of newer tasks, we define the weights  $W = \{w_j\}_{j=1}^{N_E}$  to be conditioned on the instruction tokens as

$$W = \text{Softmax}(\text{Top-}K(\mathcal{R}(\mathbf{x}_{i,\text{img}}^t, \mathbf{x}_{i,\text{text}}^t))), \quad (2)$$

where  $K$  denotes the pre-defined number of experts engaged for the translation. To provide the language model with a richer representation, we integrate the translated token from the newly selected experts with the token obtained from the pre-trained projector  $\mathcal{V}$  as

$$\tilde{\mathbf{x}}_{i,\text{img}}^t = \frac{1}{K+1} \left( \mathcal{V}(\mathbf{x}_{i,\text{img}}^t) + \sum_{j=1}^{N_E} w_j \mathcal{E}_j(\mathbf{x}_{i,\text{img}}^t) \right). \quad (3)$$

### 3.2.1. Expert Recommendation

To leverage the experts associated with old tasks that share similar visual-linguistic contexts with the new task, we introduce a recommendation strategy driven by the semantic relevance between old and new tasks. Specifically, we compute similarity scores for vision and language instructions:  $\mathbf{S}_{\text{img}}^t = \{s_{\text{img}}^{t'}\}_{t'=1}^{t-1}$ , which measures the cosine similarity between  $\mathbf{x}_{i,\text{img}}^t$  and the stored average image embedding  $\mu_{\text{img}}^{t'}$  of the  $t'$ -th previous task. Similarly, the corresponding set of textual similarity scores,  $\mathbf{S}_{\text{text}}^t = \{s_{\text{text}}^{t'}\}_{t'=1}^{t-1}$ , is computed from the current input  $\mathbf{x}_{i,\text{text}}^t$  and the stored instruction embedding  $\mu_{\text{text}}^{t'}$ <sup>1</sup>. These are combined as  $\mathbf{S}^t = \{s^{t'}\}_{t'=1}^{t-1}$ , where

$$s^{t'} = \alpha \cdot \sigma(s_{\text{img}}^{t'}) + (1 - \alpha) \cdot \sigma(s_{\text{text}}^{t'}). \quad (4)$$

$\sigma(\cdot)$  is the sigmoid function, and  $\alpha$  balances the two scores. A higher score  $s^{t'}$  indicates stronger alignment with the  $t'$ -th previous task.

Given these scores, we leverage a contrastive distribution loss [45] to encourage the outputs of the router to associate activation patterns of similar tasks while differentiating them from dissimilar ones. Let us denote the record of expert activation frequency from previous tasks by  $\bar{L}^{t'}$  and the router output for the current task by  $L^t$ , both normalized via a Softmax function. The recommendation loss becomes  $\mathcal{L}_{\text{rec}} = \sum_{i=1}^{N^t} H(\mathbf{S}^t, \pi_{t,t'})$ , where

$$\pi_{t,t'} = \frac{\exp(\text{sim}(\bar{L}^{t'}, L^t))}{\sum_{t'=1}^{t-1} \exp(\text{sim}(\bar{L}^{t'}, L^t)/\tau)}, \quad (5)$$

$H(\cdot)$  is the cross-entropy,  $\text{sim}(\cdot)$  is the cosine similarity, and  $\tau$  is the temperature parameter. By emphasizing the expert patterns that correlate with previously encountered

<sup>1</sup>  $\mu_{\text{img}}^{t'} = \text{Average}(\{x_{i,\text{img}}^{t'}\}_{i=1}^{N^{t'}})$  and  $\mu_{\text{text}}^{t'} = \text{Average}(\{x_{i,\text{text}}^{t'}\}_{i=1}^{N^{t'}})$

tasks, this recommendation encourages the router to reuse relevant expertise while minimizing reliance on less helpful ones.

**Activation Bias Reduction.** Although a mixture of experts provides flexibility in adapting to different tasks, they can lead the router to assign large weights to only a few experts [27, 43]. To mitigate such concentration, we introduce an additional regularization term that promotes diverse expert engagement by suppressing the activation of those specialized in previous tasks. We minimize

$$\mathcal{L}_{\text{bias}} = \frac{1}{2} \left( 1 + \frac{\langle \bar{L}^{1:t-1}, L^t \rangle}{\|\bar{L}^{1:t-1}\|_2 \cdot \|L^t\|_2} \right), \quad (6)$$

where  $\bar{L}^{1:t-1}$  is the normalized aggregated historical activation vector across all previous tasks.  $\langle \cdot, \cdot \rangle$  and  $\|\cdot\|_2$  denote the inner product and the  $\ell_2$  norm, respectively. This promotes the activation of a diverse set of unused experts while aligning the activations of new tasks with those from previous related tasks. To summarize, the proposed framework updates  $\mathcal{R}$  and  $\{\mathcal{E}_j\}_{j=1}^{N_E}$  by minimizing  $\mathcal{L} = \mathcal{L}_{\text{ce}} + \lambda_{\text{rec}} \mathcal{L}_{\text{rec}} + \lambda_{\text{bias}} \mathcal{L}_{\text{bias}}$ , where  $\lambda_{\text{rec}}$  and  $\lambda_{\text{bias}}$  are weighting factors for the respective losses.

### 3.2.2. Expert Pruning

A large number of previously activated experts may cause negative knowledge transfer to subsequent tasks. To alleviate the interference, we propose expert pruning on a new task after training with  $\mathcal{L}$ . We introduce a learnable vector,  $E^t = \{e_1^t, \dots, e_{N_E}^t\}$ , which is updated to limit the number of experts used for both the new and previous tasks. To discard redundant experts of the current task with sparsely activated experts, we minimize

$$\min_{E^t} \left\| \sum_{j=1}^{N_E} (w_j - e_j^t) \mathcal{E}_j(x_{i,\text{img}}^t) \right\|_F + \|\mathcal{M}^{1:t-1} + E^t\|_1, \quad (7)$$

where  $\|\cdot\|_F$  and  $\|\cdot\|_1$  denotes the Frobenius and the  $\ell_1$  norm. By minimizing the discrepancy between the output of the original expert mixture and its pruned counterpart, while constraining activation to a few experts, we identify a sparse subset of experts for the current task. The updated  $E^t$  is thresholded to produce a binary mask  $\mathcal{M}^t$ . After pruning the experts by the accumulated binary mask  $\mathcal{M}^{1:t}$ , the router is then fine-tuned to leverage the survived projectors for previous and new tasks. To collect inputs for router fine-tuning, we sample from a normal distribution defined by the stored mean and covariance of images and text instructions from observed tasks  $t' \in [1, t]$ . For each collected data, the corresponding label is sampled from  $\text{Softmax}(L^{t'} \odot \mathcal{M}^{t'})$  over the indices of experts  $1, 2, \dots, N_E$ . We minimize the cross-entropy loss to fine-tune the router.

### 3.3. Adaptive Knowledge Aggregation

Preserving the generalization capability of pre-trained models developed on extensive datasets remains critical. Our framework can effectively maintain this capability, as the proposed mixture of visual projectors is residually connected to the pre-trained projector. To this end, we present an adaptive knowledge aggregation strategy in the inference phase by leveraging the contribution of the MoE branch based on the semantic relevance of the data to previously encountered information.

Specifically, after learning the  $t$ -th task, we have the stored average visual and instruction embeddings  $\{\mu_{\text{img}}^{t'}, \mu_{\text{text}}^{t'}\}_{t'=1}^t$ . The semantic relevance is calculated as Eq.(4), yielding a combined set of scores  $\mathbf{S}_{\text{inf}}^t = \{s_{\text{inf}}^{t'}\}_{t'=1}^t$ . Intuitively, a high relevance score  $s_{\text{inf}}^{t'}$  indicates that the given vision-instruction paired data is more likely associated with the  $t'$ -th task. Consequently, the translated visual token for the language model is represented as a linear combination of the pre-trained projection and the MoE-translated projection, weighted by  $\lambda_{\text{inf}} = \text{argmax}_{t' \in [1, t]} \{s_{\text{inf}}^{t'}\}_{t'=1}^t$ , as

$$\frac{1}{\lambda_{\text{inf}} \cdot K + 1} \left( \mathcal{V}(\mathbf{x}_{i, \text{img}}^{\text{inf}}) + \lambda_{\text{inf}} \sum_{j=1}^{N_E} w_j \mathcal{E}_j(\mathbf{x}_{i, \text{img}}^{\text{inf}}) \right), \quad (8)$$

where  $\mathbf{x}_{i, \text{img}}^{\text{inf}}$  denotes an input for inference and the weighting factor  $\lambda_{\text{inf}}$  ranges in  $[0, 1]$ . This adaptive aggregation ensures that the model retains its inherent zero-shot generalization capacity for unseen samples by calibrating the contributions of MoE-derived knowledge.

## 4. Experiments

### 4.1. Experimental Setting

**Datasets.** We applied the proposed Mixture-of-Visual Projectors, named MVP, to continual learning of diverse vision-language tasks; image classification [17], image captioning [39], and image question answering [42]. For classification, we employed the ImageNet-R dataset [17] widely used in continual learning [44, 47]. The dataset was divided into 10 subsets containing 20 classes each, following the previous practices [44, 47]. We used Flickr-30K [39] for captioning tasks. We divided the dataset into four subsets based on the type of visual categories [12]: animals, instruments, scenes, and vehicles. For question answering, we employed the COCO-QA dataset [42]. We divided the dataset into four distinct subsets based on the type of language instructions [53]: object, count, color, and position. We define each subset as a task and train one task at each time step, which results in a sequence of 18 tasks.

**Evaluation metrics.** To evaluate the proposed method, we employ three metrics [50, 54]: *Last*, *Transfer*, and *Avg*.

*Last* calculates the final performance after training all tasks. *Transfer* measures the models' zero-shot performance on unseen tasks. *Avg* is the average performance across all time steps. For classification and question answering tasks, we reported the metrics based on the accuracy of generated responses. For captioning tasks, the performance is evaluated by the RefCLIP-Score [18]. To enhance interpretability, we scaled the score, which ranges from 0 to 1. Please refer to the supplementary materials for measuring the accuracy of the generated responses.

**Implementation details.** We adopted Vicuna-7B [9] as the language decoder and employed the pre-trained ViT-g/14 [14] in conjunction with the Qformer as the visual encoder, following the practice in [4]. Additionally, we employed another VLM that utilized LLaMa-2-7B [46] as the language decoder and the visual encoder [14] without Qformer. We initialized the experts of the proposed method using the pre-trained visual projectors of VLMs, provided in [55]. We set the number of experts  $N_E$  to 20,  $K$  to 2, semantic score parameter  $\alpha$  to 0.3, and the loss weights  $\lambda_{\text{rec}}$  and  $\lambda_{\text{bias}}$  to 1 for all experiments. The proposed method was trained using the Adam optimizer with  $\beta_1$  and  $\beta_2$  of 0.9 and 0.999. All experiments were conducted using NVIDIA RTX 3090 GPUs. For additional details, please refer to the supplementary material.

**Comparison methods.** To evaluate the proposed method, we compared it with existing continual learning methods, including conventional methods, LwF [30], EWC [25], and MoEAdapter [50], and the methods for VLMs, GMM [4] and EProj [16]. All comparison methods employed the same pre-trained VLMs and froze the visual and language encoders while training the visual projector for tasks. For the MoE-based continual learning method [50], we utilized its routing scheme and set its expert as the visual projector. Additionally, we reported the zero-shot performance of the pre-trained model, referred to as Zero-Shot.

### 4.2. Comparison Results

We evaluated the proposed method and the comparison methods on diverse vision-language tasks learned in the order of classification, captioning, and question answering. Table 1 shows the experimental results of continual learning methods using Vicuna as a large language model. Overall, the proposed method outperforms other continual learning methods in terms of the *Last*, *Avg*, and *Transfer* metrics across most tasks. The existing methods, LwF, EWC, GMM, and EProj, show unsatisfactory performance measured with *Last* due to overwriting previously learned knowledge in a shared projector across tasks by the latest learned question answering task. The proposed method, MVP, achieves superior classification performance, with notable performance gaps ranging from 12.80% to 75.71% compared to EProj and MoEAdapter. These results high-

Table 1. Results of the compared methods that employed Vicuna were measured using the *Last*, *Avg*, and *Transfer* metrics. The classification results were averaged across tasks. The names of the captioning and question answering tasks are abbreviated based on their visual and instruction types, respectively.

Method	Classification (Accuracy)			Captioning (RefCLIP-Score)				Question Answering (Accuracy)			
	$T^1$ - $T^3$	$T^4$ - $T^6$	$T^7$ - $T^{10}$	Anim.	Inst.	Scen.	Vehi.	Obje.	Coun.	Colo.	Posi.
<b>Vicuna</b>											
Zero-Shot	67.79	63.16	62.87	77.08	75.24	74.24	73.43	68.52	42.55	62.62	32.79
<b>Last</b>											
LwF [30]	4.38	4.77	5.83	70.16	70.31	70.15	68.60	70.69	65.45	76.46	59.51
EWC [25]	5.61	6.80	5.83	67.00	67.39	66.13	66.47	65.72	63.63	73.69	44.13
GMM [4]	1.33	0.94	1.62	62.96	61.08	63.73	64.70	42.29	46.23	45.11	25.74
EProj [16]	8.50	12.82	11.81	73.78	71.43	72.39	72.23	39.77	60.00	65.84	24.69
MoEAdapter [50]	70.01	65.10	65.55	76.53	76.23	76.43	73.92	66.76	42.18	41.53	38.86
MVP (Ours)	<b>82.81</b>	<b>85.34</b>	<b>87.52</b>	<b>79.60</b>	<b>77.57</b>	<b>76.06</b>	<b>77.79</b>	<b>79.26</b>	<b>74.54</b>	<b>80.30</b>	<b>71.25</b>
<b>Avg</b>											
LwF [30]	48.37	49.42	51.62	70.63	70.34	68.56	69.18	53.99	47.21	60.22	37.51
EWC [25]	55.21	50.13	52.74	72.18	72.72	71.86	71.64	52.56	48.74	56.45	27.08
GMM [4]	43.92	42.08	50.70	69.62	69.15	68.84	68.80	48.39	48.18	48.47	27.71
EProj [16]	49.18	45.55	48.23	73.78	71.43	72.39	72.23	40.06	<b>50.88</b>	50.65	21.68
MoEAdapter [50]	71.50	67.16	66.27	76.65	75.97	74.40	74.66	67.95	42.60	53.82	36.48
MVP (Ours)	<b>81.34</b>	<b>82.03</b>	<b>85.07</b>	<b>78.71</b>	<b>76.92</b>	<b>75.92</b>	<b>76.25</b>	<b>70.16</b>	50.68	<b>71.34</b>	<b>38.55</b>
<b>Transfer</b>											
LwF [30]	69.68	64.30	71.26	67.15	67.97	66.74	68.41	49.07	43.80	58.47	36.17
EWC [25]	71.85	66.81	75.69	74.00	72.85	72.65	72.63	48.57	45.33	54.20	26.07
GMM [4]	74.59	65.82	81.96	70.40	70.30	69.84	69.77	42.29	46.23	45.11	25.74
EProj [16]	71.85	66.81	75.76	73.98	72.34	72.06	71.86	42.17	<b>48.99</b>	48.65	21.50
MoEAdapter [50]	75.01	66.61	67.05	76.80	75.80	74.38	74.94	68.29	42.69	55.35	36.34
MVP (Ours)	<b>77.95</b>	<b>73.34</b>	<b>82.52</b>	<b>78.02</b>	<b>76.88</b>	<b>75.71</b>	<b>75.91</b>	<b>67.52</b>	45.89	<b>70.17</b>	<b>36.62</b>

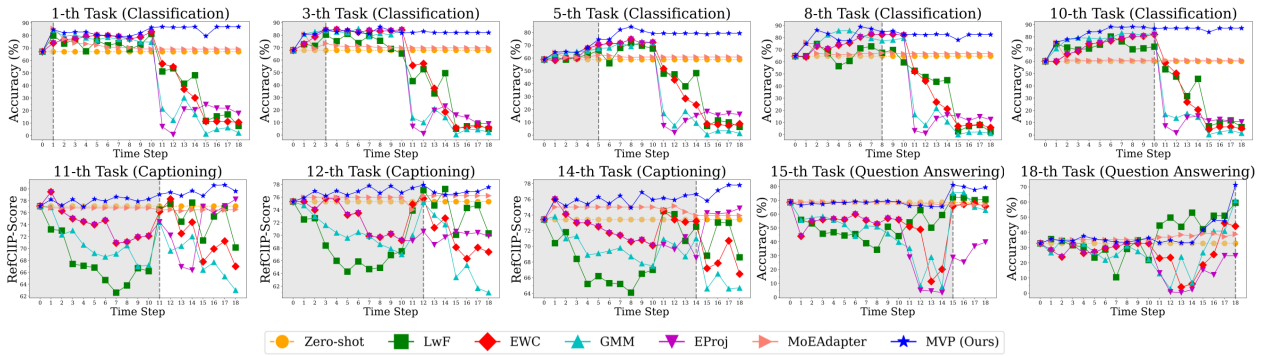


Figure 3. Performance of each task across time steps. The gray area represents the time steps preceding training for specific tasks, and the vertical dashed line indicates the time step at which the corresponding task is learned. Best viewed in color ( $\times 2$ ).

light the importance of instruction context-aware translation in continual learning for VLMs.

Note that most compared methods using a shared visual projector, which tends to overfit on classification, achieve higher performance than Zero-Shot in *Transfer* but exhibit a significant performance drop in captioning and question answering tasks. In contrast, MVP achieves higher performance than Zero-Shot in most tasks, demonstrating that the relevance-based expert recommendation and knowledge aggregation contribute to effective context-aware translation. For the results of a different task order, please refer to the supplementary material.

We also present the performance of tasks at each time in Figure 3. As shown in the figure (top), most methods show improved performance on subsequent classification tasks

after training on the other classification tasks. However, their performance significantly degrades after training on captioning and question answering tasks, with results lower than the zero-shot performance of the pre-trained model (indicated by the yellow horizontal line). The performance of captioning tasks decreases when newer tasks are introduced, with this decline becoming more pronounced following the introduction of the question answering tasks. In contrast, the proposed approach does not exhibit a performance drop in each task after learning other tasks. Notably, the performance of captioning tasks shows a slight improvement after learning classification tasks. This is attributed to the instruction-grounded translator that leverages knowledge of classification to help perform captioning tasks.

Table 2. Results of using VLM with LLaMa-2.  $\Delta$  indicates the performance gap with the pre-trained VLM. Average indicates the average performance of tasks.

Method	Classification		Captioning		Question Answering	
	Average	$\Delta$ ( $\uparrow$ )	Average	$\Delta$ ( $\uparrow$ )	Average	$\Delta$ ( $\uparrow$ )
<b>LLaMa-2</b>						
Zero-Shot	59.21	0.00	75.90	0.00	60.31	0.00
<b>Last</b>						
LwF [30]	70.13	+10.92	77.12	+1.22	54.79	-5.52
EWC [25]	52.55	-6.66	68.87	-7.03	31.60	-28.71
GMM [4]	21.28	-37.93	78.92	+3.02	59.48	-0.83
EProj [16]	53.68	-5.53	66.42	-9.48	30.44	-29.87
MoEAdapter [50]	61.30	+2.09	75.87	-0.03	59.26	-1.05
<b>MVP (Ours)</b>	<b>79.99</b>	<b>+20.78</b>	<b>78.72</b>	<b>+2.82</b>	<b>67.46</b>	<b>+7.15</b>
<b>Avg</b>						
LwF [30]	68.02	+8.81	73.50	-2.40	49.92	-10.39
EWC [25]	48.91	-10.30	65.57	-10.33	35.31	-25.00
GMM [4]	64.20	+4.99	73.31	-2.59	50.13	-10.18
EProj [16]	49.74	-9.47	64.61	-11.29	32.82	-27.49
MoEAdapter [50]	62.77	+3.56	75.87	-0.03	60.16	-0.15
<b>MVP (Ours)</b>	<b>78.58</b>	<b>+19.37</b>	<b>78.37</b>	<b>+2.47</b>	<b>61.66</b>	<b>+1.35</b>
<b>Transfer</b>						
LwF [30]	63.88	+4.67	71.81	-4.09	49.07	-11.24
EWC [25]	47.33	-11.88	64.24	-11.66	37.36	-22.95
GMM [4]	49.74	-9.47	64.61	-11.29	32.82	-27.49
EProj [16]	47.11	-12.10	63.92	-11.98	34.19	-26.12
MoEAdapter [50]	65.15	+5.94	75.08	-0.82	56.27	-4.04
<b>MVP (Ours)</b>	<b>74.39</b>	<b>+15.18</b>	<b>77.67</b>	<b>+1.77</b>	<b>57.16</b>	<b>-3.15</b>

To evaluate the proposed method based on another VLM, we conducted additional experiments using LLaMa-2 [46], which has a different language decoder and a vision encoder compared to the previous VLM using Vicuna. Table 2 shows the results of the methods with the same task order as in Table 1. The trends of the results are similar to those in Table 1. Most competitors underperform Zero-Shot in *Last*, whereas MVP outperforms Zero-Shot by large average margins of 20.78%, 2.82, and 7.15% in classification, captioning, and question answering, respectively. MVP also outperforms the runner-up method, MoEAdapter, in *Transfer* by 9.24%, 2.59, and 0.89% across the tasks. This results from relevance-based calibration of newly acquired and pre-trained knowledge, unlike MoEAdapter, which relies solely on pre-trained knowledge for unseen tasks.

### 4.3. Ablation Study and Analysis

**Ablation study.** We conducted an ablation study by sequentially removing key components: visual projectors, recommendation loss  $\mathcal{L}_{rec}$ , activation bias reduction loss  $\mathcal{L}_{bias}$ , expert pruning, and adaptive knowledge aggregation (AKA). Table 3 shows the results of the ablation study. The method without AKA degrades not only *Transfer* but also *Last* compared to that with AKA, demonstrating the importance of calibrating learned knowledge based on semantic relevance. The method without pruning degrades the average performance of captioning (76.70 to 71.55) and question answering (76.17% to 75.54%) in *Last*, indicating that pruning helps to mitigate negative transfer by eliminating redundant experts. We also observe that the method with-

Table 3. Ablation study of MVP with different components.

Method	Classification		Captioning		Question Answering	
	Average	$\Delta$ ( $\uparrow$ )	Average	$\Delta$ ( $\uparrow$ )	Average	$\Delta$ ( $\uparrow$ )
<b>Vicuna</b>						
Zero-shot	64.41	0.00	75.00	0.00	51.62	0.00
<b>Last</b>						
MVP (Complete method)	85.87	+21.46	77.75	+2.75	76.34	+24.72
w/o AKA	85.53	+21.12	76.70	+1.70	76.17	+24.55
w/o AKA, Prune	85.92	+21.51	71.55	-3.45	75.54	+23.92
w/o AKA, Prune, $\mathcal{L}_{bias}$	3.31	-61.10	70.70	-4.30	73.99	+22.37
w/o AKA, Prune, $\mathcal{L}_{bias}$ , $\mathcal{L}_{rec}$	0.25	-64.16	68.51	-6.49	74.53	+22.91
w/o all (Single projector [4])	1.49	-62.92	63.10	-11.90	60.15	+8.53
<b>Avg</b>						
MVP (Complete method)	83.28	+18.87	76.94	+1.94	57.68	+6.06
w/o AKA	83.02	+18.61	72.21	-2.79	48.64	-2.98
w/o AKA, Prune	83.51	+19.10	69.22	-5.78	47.05	-4.57
w/o AKA, Prune, $\mathcal{L}_{bias}$	69.59	+5.18	71.60	-3.40	51.68	+0.06
w/o AKA, Prune, $\mathcal{L}_{bias}$ , $\mathcal{L}_{rec}$	58.51	-5.90	70.59	-4.41	51.39	-0.23
w/o all (Single projector [4])	46.97	-17.44	69.10	-5.90	43.10	-8.52
<b>Transfer</b>						
MVP (Complete method)	78.45	+14.04	76.16	+1.16	50.89	-0.73
w/o AKA	78.40	+13.99	68.92	-6.08	44.55	-7.07
w/o AKA Prune	78.34	+13.93	68.78	-6.22	43.03	-8.59
w/o AKA, Prune, $\mathcal{L}_{bias}$	78.06	+13.65	71.47	-3.53	47.94	-3.68
w/o AKA, Prune, $\mathcal{L}_{bias}$ , $\mathcal{L}_{rec}$	78.26	+13.85	70.45	-4.55	47.68	-3.94
w/o all (Single projector [4])	76.31	+11.90	69.97	-5.03	39.03	-12.59

out AKA and pruning shows slightly lower performance in *Transfer* than the approach that also removes  $\mathcal{L}_{bias}$ , as a diverse set of activated experts for seen tasks is repurposed for unseen tasks. However, the methods using  $\mathcal{L}_{bias}$  yield substantial improvement compared to the method without it in *Last*, especially in classification (3.31% to 85.92%), by promoting diversified experts utilization. Additionally, the methods without  $\mathcal{L}_{rec}$  shows performance drop measured in *Avg*, particularly in classification ( $\Delta$  +5.18 to -5.90) and question answering ( $\Delta$  +0.06 to -0.23).

**Qualitative results.** To investigate the changes in responses throughout the continual learning process, we provide a qualitative analysis. Figure 4 shows generated responses over time steps from different continual learning methods using Vicuna. The proposed method generates responses that reflect the given instruction for the visual input while maintaining the response quality similar to zero-shot performance, even before learning the task associated with the given image-instruction pair. In contrast, LwF and GMM often neglect the language instruction and forget previously learned detailed visual information, generating coarse-grained responses (e.g., “a drawing” for classification and “car” for captioning as shown in Figure 4). By leveraging the instruction-aware visual projectors, MVP generates specialized responses for learned tasks and responses similar to zero-shot performance for unseen tasks.

**Expert activation frequency.** We further analyze the combinations of three components, recommendation loss, activation bias reduction loss, and expert pruning, that influence the expert activation pattern, as in Figure 5. When only the recommendation loss is applied, a limited subset of experts is predominantly activated (similar observations in [27, 43]). In contrast, combining recommendation with

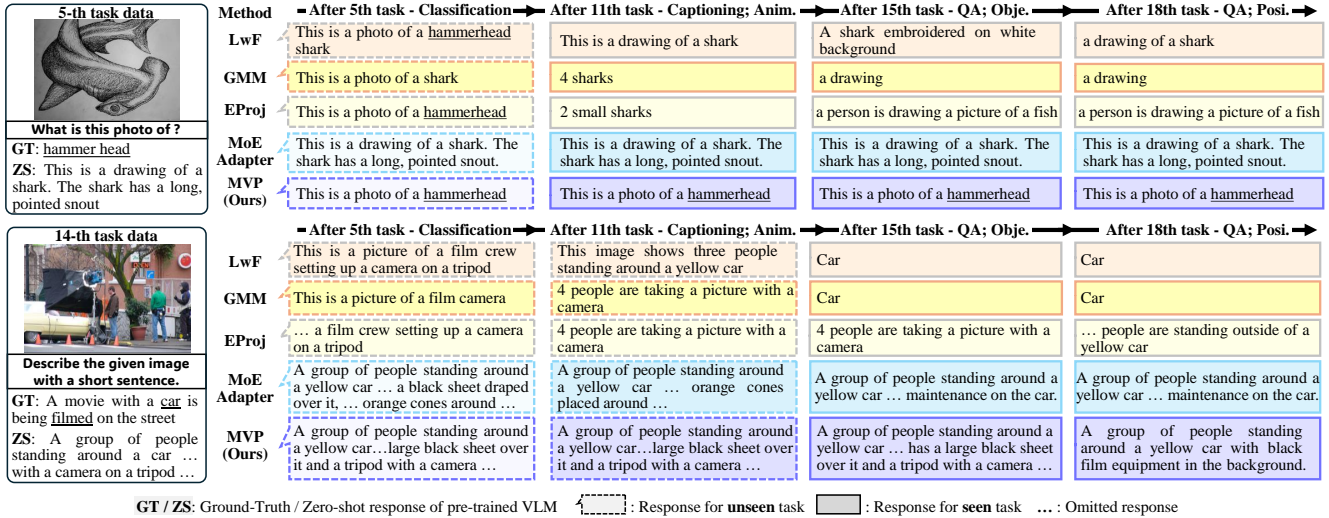


Figure 4. Qualitative results of the continual learning methods illustrating changes of responses to randomly selected samples after learning of newly emerging tasks. The proposed method generates consistent responses after learning other tasks, preserving both detailed category knowledge (top) and overall scene perception (bottom).

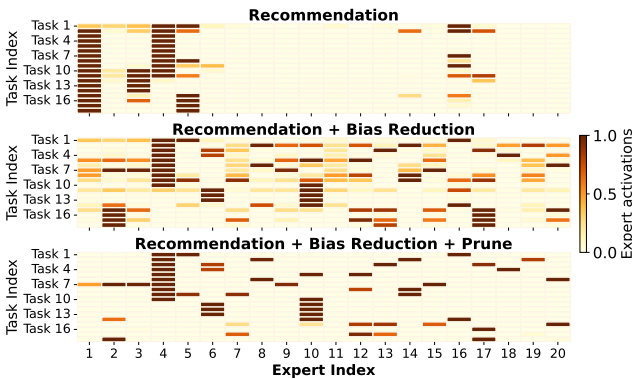


Figure 5. Results of expert activation frequency for each task by ablating the components of MVP.

the activation bias reduction loss promotes broader expert activation. Notably, expert activation frequencies change at task transitions, particularly from classification to captioning (task index 11) and from captioning to question answering (task index 15).

**Impact of the number of experts.** We conducted additional experiments by varying the number of visual projectors in the proposed method. The results presented in Figure 6 indicate that using a small number of experts (one or two) leads to a considerable degradation in performance. In contrast, incorporating three or more experts yields performance improvements and suggests that the additional experts provide sufficient capacity for tasks with novel language instructions. Please refer to the supplementary material for additional results on varying text instructions, computational cost, and generative VLM benchmark [28].

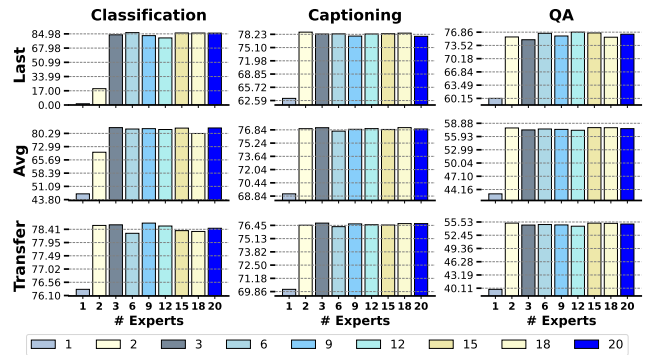


Figure 6. Results for MVP with varying numbers of experts.

## 5. Conclusion

In this paper, we have proposed a novel continual learning framework for generative vision-language models that adaptively translate visual information grounded on language instructions. We have introduced a mixture of visual projectors to leverage an appropriate visual translator based on the context of the given instruction and visual information. To mitigate the use of projectors across different contexts, we have proposed a semantic relevance-guided expert recommendation strategy that promotes the sparse activation of experts relevant to previous tasks while suppressing negative knowledge transfer. Extensive experiments on a challenging sequence of tasks, including image classification, captioning, and question answering, demonstrate that the proposed method outperforms other continual learning methods on both seen and unseen tasks.

**Acknowledgement.** This work was supported in part by the National Research Foundation of Korea (NRF) grant funded by the Korea government (MSIT) (RS-2023-00279019) and in part by the Institute of Information & Communications Technology Planning & Evaluation (IITP) grant funded by the Korea government (MSIT) (RS-2021-II211341, Artificial Intelligence Graduate School Program (Chung-Ang University)).

## References

- [1] Josh Achiam, Steven Adler, Sandhini Agarwal, Lama Ahmad, Ilge Akkaya, Florencia Leoni Aleman, Diogo Almeida, Janko Altenschmidt, Sam Altman, Shyamal Anadkat, et al. GPT-4 technical report. *arXiv preprint arXiv:2303.08774*, 2023. 1, 2
- [2] Rahaf Aljundi, Punarjay Chakravarty, and Tinne Tuytelaars. Expert gate: Lifelong learning with a network of experts. In *Proceedings of the IEEE Conference on Computer Vision and Pattern Recognition*, pages 3366–3375, 2017. 2
- [3] Rahaf Aljundi, Francesca Babiloni, Mohamed Elhoseiny, Marcus Rohrbach, and Tinne Tuytelaars. Memory aware synapses: Learning what (not) to forget. In *European Conference on Computer Vision*, pages 144–161. Springer, 2018. 2
- [4] Xusheng Cao, Haori Lu, Linlan Huang, Xialei Liu, and Ming-Ming Cheng. Generative multi-modal models are good class incremental learners. In *Proceedings of the IEEE/CVF Conference on Computer Vision and Pattern Recognition*, pages 28706–28717, 2024. 1, 2, 3, 5, 6, 7
- [5] Junbum Cha, Wooyoung Kang, Jonghwan Mun, and Byungseok Roh. Honeybee: Locality-enhanced projector for multimodal llm. In *Proceedings of the IEEE/CVF Conference on Computer Vision and Pattern Recognition*, pages 13817–13827, 2024. 2
- [6] Arslan Chaudhry, Puneet K Dokania, Thalaiyasingam Ajanthan, and Philip HS Torr. Riemannian walk for incremental learning: Understanding forgetting and intransigence. In *European Conference on Computer Vision*, pages 556–572. Springer, 2018. 2
- [7] Cheng Chen, Junchen Zhu, Xu Luo, Hengtao Shen, Jingkuan Song, and Lianli Gao. CoIN: A benchmark of continual instruction tuning for multimodal large language models. *Advances in Neural Information Processing Systems*, 37: 57817–57840, 2025. 1
- [8] Wuyang Chen, Yanqi Zhou, Nan Du, Yanping Huang, James Laudon, Zhifeng Chen, and Claire Cui. Lifelong language pretraining with distribution-specialized experts. In *International Conference on Machine Learning*, pages 5383–5395. PMLR, 2023. 2
- [9] Wei-Lin Chiang, Zhuohan Li, Zi Lin, Ying Sheng, Zhanghao Wu, Hao Zhang, Lianmin Zheng, Siyuan Zhuang, Yonghao Zhuang, Joseph E Gonzalez, et al. Vicuna: An open-source chatbot impressing gpt-4 with 90%\* chatgpt quality, march 2023. URL <https://lmsys.org/blog/2023-03-30-vicuna>, 3(5), 2023. 2, 5
- [10] Alessandro Conti, Enrico Fini, Massimiliano Mancini, Paolo Rota, Yiming Wang, and Elisa Ricci. Vocabulary-free image classification. *Advances in Neural Information Processing Systems*, 36:30662–30680, 2023. 1
- [11] Wenliang Dai, Junnan Li, D Li, AMH Tiong, J Zhao, W Wang, B Li, P Fung, and S Hoi. Instructblip: Towards general-purpose vision-language models with instruction tuning. arxiv 2023. *arXiv preprint arXiv:2305.06500*, 2, 2023. 2
- [12] Riccardo Del Chiaro, Bartłomiej Twardowski, Andrew Bagdanov, and Joost Van de Weijer. RATT: Recurrent attention to transient tasks for continual image captioning. *Advances in Neural Information Processing Systems*, 33:16736–16748, 2020. 5
- [13] Arthur Douillard, Alexandre Ramé, Guillaume Couairon, and Matthieu Cord. DyTox: Transformers for continual learning with dynamic token expansion. In *Proceedings of the IEEE/CVF Conference on Computer Vision and Pattern Recognition*, pages 9285–9295, 2022. 1, 2
- [14] Yuxin Fang, Wen Wang, Binhui Xie, Quan Sun, Ledell Wu, Xinggang Wang, Tiejun Huang, Xinlong Wang, and Yue Cao. EVA: Exploring the limits of masked visual representation learning at scale. In *Proceedings of the IEEE/CVF Conference on Computer Vision and Pattern Recognition*, pages 19358–19369, 2023. 5
- [15] Xinyuan Gao, Songlin Dong, Yuhang He, Qiang Wang, and Yihong Gong. Beyond prompt learning: Continual adapter for efficient rehearsal-free continual learning. In *European Conference on Computer Vision*, pages 89–106, 2024. 2
- [16] Jinghan He, Haiyun Guo, Ming Tang, and Jinqiao Wang. Continual instruction tuning for large multimodal models. *arXiv preprint arXiv:2311.16206*, 2023. 1, 3, 5, 6, 7
- [17] Dan Hendrycks, Steven Basart, Norman Mu, Saurav Kadavath, Frank Wang, Evan Dorundo, Rahul Desai, Tyler Zhu, Samyak Parajuli, Mike Guo, et al. The many faces of robustness: A critical analysis of out-of-distribution generalization. In *Proceedings of the IEEE/CVF international conference on computer vision*, pages 8340–8349, 2021. 2, 5
- [18] Jack Hessel, Ari Holtzman, Maxwell Forbes, Ronan Le Bras, and Yejin Choi. CLIPScore: A reference-free evaluation metric for image captioning. In *Proceedings of the 2021 Conference on Empirical Methods in Natural Language Processing*, pages 7514–7528, 2021. 5
- [19] Edward J Hu, Yelong Shen, Phillip Wallis, Zeyuan Allen-Zhu, Yuanzhi Li, Shean Wang, Lu Wang, and Weizhu Chen. LoRA: Low-rank adaptation of large language models. *arXiv preprint arXiv:2106.09685*, 2021. 2
- [20] Robert A Jacobs, Michael I Jordan, Steven J Nowlan, and Geoffrey E Hinton. Adaptive mixtures of local experts. *Neural computation*, 3(1):79–87, 1991. 2
- [21] Menglin Jia, Luming Tang, Bor-Chun Chen, Claire Cardie, Serge Belongie, Bharath Hariharan, and Ser-Nam Lim. Visual prompt tuning. In *European Conference on Computer Vision*, pages 709–727. Springer, 2022. 2
- [22] Hyundong Jin and Eunwoo Kim. Helpful or harmful: Inter-task association in continual learning. In *European conference on computer vision*, pages 519–535. Springer, 2022. 1
- [23] Hyundong Jin, Gyeong-hyeon Kim, Chanho Ahn, and Eunwoo Kim. Growing a brain with sparsity-inducing generation for continual learning. In *Proceedings of the IEEE/CVF*

- international conference on computer vision*, pages 18961–18970, 2023. 1
- [24] Andrej Karpathy and Li Fei-Fei. Deep visual-semantic alignments for generating image descriptions. In *Proceedings of the IEEE conference on computer vision and pattern recognition*, pages 3128–3137, 2015. 1
- [25] James Kirkpatrick, Razvan Pascanu, Neil Rabinowitz, Joel Veness, Guillaume Desjardins, Andrei A Rusu, Kieran Milan, John Quan, Tiago Ramalho, Agnieszka Grabska-Barwinska, et al. Overcoming catastrophic forgetting in neural networks. *Proceedings of the National Academy of Sciences of the United States of America*, 114(13):3521–3526, 2017. 1, 2, 5, 6, 7
- [26] Alexandre Lacoste, Alexandra Luccioni, Victor Schmidt, and Thomas Dandres. Quantifying the carbon emissions of machine learning. *arXiv preprint arXiv:1910.09700*, 2019. 1
- [27] Dmitry Lepikhin, HyoukJoong Lee, Yuanzhong Xu, Dehao Chen, Orhan Firat, Yanping Huang, Maxim Krikun, Noam Shazeer, and Zhifeng Chen. GShard: Scaling giant models with conditional computation and automatic sharding. In *International Conference on Learning Representations*. 4, 7
- [28] Bohao Li, Rui Wang, Guangzhi Wang, Yuying Ge, Yixiao Ge, and Ying Shan. Seed-bench: Benchmarking multimodal llms with generative comprehension. *arXiv preprint arXiv:2307.16125*, 2023. 8, 3
- [29] Junnan Li, Dongxu Li, Silvio Savarese, and Steven Hoi. BLIP-2: Bootstrapping language-image pre-training with frozen image encoders and large language models. In *International conference on machine learning*, pages 19730–19742. PMLR, 2023. 2
- [30] Zhizhong Li and Derek Hoiem. Learning without forgetting. *IEEE transactions on pattern analysis and machine intelligence*, 40(12):2935–2947, 2017. 5, 6, 7, 1
- [31] Yan-Shuo Liang and Wu-Jun Li. InfLoRA: Interference-free low-rank adaptation for continual learning. In *Proceedings of the IEEE/CVF Conference on Computer Vision and Pattern Recognition*, pages 23638–23647, 2024. 1
- [32] Haotian Liu, Chunyuan Li, Yuheng Li, and Yong Jae Lee. Improved baselines with visual instruction tuning. In *Proceedings of the IEEE/CVF Conference on Computer Vision and Pattern Recognition*, pages 26296–26306, 2024. 2
- [33] Haotian Liu, Chunyuan Li, Qingyang Wu, and Yong Jae Lee. Visual instruction tuning. *Advances in neural information processing systems*, 36, 2024. 1
- [34] Yaoyao Liu, Bernt Schiele, and Qianru Sun. Adaptive aggregation networks for class-incremental learning. In *The IEEE/CVF Conference on Computer Vision and Pattern Recognition (CVPR)*, pages 2544–2553, 2021. 2
- [35] Jiasen Lu, Christopher Clark, Sangho Lee, Zichen Zhang, Savya Khosla, Ryan Marten, Derek Hoiem, and Aniruddha Kembhavi. Unified-IO 2: Scaling autoregressive multimodal models with vision language audio and action. In *Proceedings of the IEEE/CVF Conference on Computer Vision and Pattern Recognition*, pages 26439–26455, 2024. 1
- [36] Xudong Lu, Qi Liu, Yuhui Xu, Aojun Zhou, Siyuan Huang, Bo Zhang, Junchi Yan, and Hongsheng Li. Not all experts are equal: Efficient expert pruning and skipping for mixture-of-experts large language models. In *Proceedings of the 62nd Annual Meeting of the Association for Computational Linguistics (Volume 1: Long Papers)*, pages 6159–6172, Bangkok, Thailand, 2024. Association for Computational Linguistics. 2, 1
- [37] Michael McCloskey and Neal J Cohen. Catastrophic interference in connectionist networks: The sequential learning problem. In *Psychology of learning and motivation*, pages 109–165. Elsevier, 1989. 1, 2
- [38] Basil Mustafa, Carlos Riquelme, Joan Puigcerver, Rodolphe Jenatton, and Neil Houlsby. Multimodal contrastive learning with limoe: the language-image mixture of experts. *Advances in Neural Information Processing Systems*, 35:9564–9576, 2022. 2
- [39] Bryan A Plummer, Liwei Wang, Chris M Cervantes, Juan C Caicedo, Julia Hockenmaier, and Svetlana Lazebnik. Flickr30k entities: Collecting region-to-phrase correspondences for richer image-to-sentence models. *International Journal of Computer Vision*, 123:74–93, 2017. 2, 5
- [40] Alec Radford, Jong Wook Kim, Chris Hallacy, Aditya Ramesh, Gabriel Goh, Sandhini Agarwal, Girish Sastry, Amanda Askell, Pamela Mishkin, Jack Clark, et al. Learning transferable visual models from natural language supervision. In *International conference on machine learning*, pages 8748–8763. PMLR, 2021. 1
- [41] Sylvestre-Alvise Rebuffi, Alexander Kolesnikov, Georg Sperl, and Christoph H Lampert. iCaRL: Incremental classifier and representation learning. In *Proceedings of the IEEE conference on Computer Vision and Pattern Recognition*, pages 2001–2010, 2017. 1, 2
- [42] Mengye Ren, Ryan Kiros, and Richard Zemel. Exploring models and data for image question answering. *Advances in neural information processing systems*, 28, 2015. 1, 2, 5
- [43] Noam Shazeer, Azalia Mirhoseini, Krzysztof Maziarz, Andy Davis, Quoc Le, Geoffrey Hinton, and Jeff Dean. Outrageously large neural networks: The sparsely-gated mixture-of-experts layer. *arXiv preprint arXiv:1701.06538*, 2017. 4, 7
- [44] James Seale Smith, Leonid Karlinsky, Vyshnavi Gutta, Paola Cascante-Bonilla, Donghyun Kim, Assaf Arbelle, Rameswar Panda, Rogerio Feris, and Zsolt Kira. CODA-prompt: Continual decomposed attention-based prompting for rehearsal-free continual learning. In *Proceedings of the IEEE/CVF Conference on Computer Vision and Pattern Recognition*, pages 11909–11919, 2023. 1, 2, 5
- [45] Yu Tian, Guansong Pang, Fengbei Liu, Yuanhong Chen, Seon Ho Shin, Johan W Verjans, Rajvinder Singh, and Gustavo Carneiro. Constrained contrastive distribution learning for unsupervised anomaly detection and localisation in medical images. In *Medical Image Computing and Computer Assisted Intervention—MICCAI 2021: 24th International Conference, Strasbourg, France, September 27–October 1, 2021, Proceedings, Part V 24*, pages 128–140. Springer, 2021. 4
- [46] Hugo Touvron, Louis Martin, Kevin Stone, Peter Albert, Amjad Almahairi, Yasmine Babaei, Nikolay Bashlykov, Soumya Batra, Prajjwal Bhargava, Shruti Bhosale, et al. Llama 2: Open foundation and fine-tuned chat models. *arXiv preprint arXiv:2307.09288*, 2023. 2, 5, 7

- [47] Zifeng Wang, Zizhao Zhang, Sayna Ebrahimi, Ruoxi Sun, Han Zhang, Chen-Yu Lee, Xiaoqi Ren, Guolong Su, Vincent Perot, Jennifer Dy, et al. DualPrompt: Complementary prompting for rehearsal-free continual learning. In *European Conference on Computer Vision*, pages 631–648. Springer, 2022. [2](#), [5](#)
- [48] Zifeng Wang, Zizhao Zhang, Chen-Yu Lee, Han Zhang, Ruoxi Sun, Xiaoqi Ren, Guolong Su, Vincent Perot, Jennifer Dy, and Tomas Pfister. Learning to prompt for continual learning. In *Proceedings of the IEEE/CVF conference on computer vision and pattern recognition*, pages 139–149, 2022. [1](#), [2](#)
- [49] Qinghao Ye, Haiyang Xu, Guohai Xu, Jiabo Ye, Ming Yan, Yiyang Zhou, Junyang Wang, Anwen Hu, Pengcheng Shi, Yaya Shi, et al. mPLUG-OWL: Modularization empowers large language models with multimodality. *arXiv preprint arXiv:2304.14178*, 2023. [2](#)
- [50] Jiazuo Yu, Yunzhi Zhuge, Lu Zhang, Ping Hu, Dong Wang, Huchuan Lu, and You He. Boosting continual learning of vision-language models via mixture-of-experts adapters. In *Proceedings of the IEEE/CVF Conference on Computer Vision and Pattern Recognition*, pages 23219–23230, 2024. [2](#), [5](#), [6](#), [7](#), [1](#)
- [51] Friedemann Zenke, Ben Poole, and Surya Ganguli. Continual learning through synaptic intelligence. In *Proceedings of the 34th International Conference on Machine Learning-Volume 70*, pages 3987–3995, 2017. [2](#)
- [52] Yuexiang Zhai, Shengbang Tong, Xiao Li, Mu Cai, Qing Qu, Yong Jae Lee, and Yi Ma. Investigating the catastrophic forgetting in multimodal large language models. In *NeurIPS 2023 Workshop on Instruction Tuning and Instruction Following*. [2](#)
- [53] Yue Zhang, Hehe Fan, and Yi Yang. Prompt-aware adapter: Towards learning adaptive visual tokens for multimodal large language models. *arXiv preprint arXiv:2405.15684*, 2024. [5](#)
- [54] Zangwei Zheng, Mingyuan Ma, Kai Wang, Ziheng Qin, Xiangyu Yue, and Yang You. Preventing zero-shot transfer degradation in continual learning of vision-language models. In *Proceedings of the IEEE/CVF International Conference on Computer Vision*, pages 19125–19136, 2023. [5](#)
- [55] Deyao Zhu, Jun Chen, Xiaoqian Shen, Xiang Li, and Mohamed Elhoseiny. MiniGPT-4: Enhancing vision-language understanding with advanced large language models. *arXiv preprint arXiv:2304.10592*, 2023. [1](#), [2](#), [5](#)

# Instruction-Grounded Visual Projectors for Continual Learning of Generative Vision-Language Models

## Supplementary Material

### A. Additional Implementation Details

**Details of Router.** We concatenated the image feature and instruction token and used them as input to the router. To align the dimension of the image feature with that of the instruction token, we first applied a pre-trained visual projector to the image feature. To more effectively extract contextual information from the given instructions, we employed a simple linguistic preprocessing technique, following [10]. Specifically, we applied Part-of-Speech (POS) tagging to categorize key components, such as WH-words, nouns, and verbs, while filtering out irrelevant terms. The filtered instructions were then processed through the tokenizer and embedding function of a pre-trained model to extract text tokens for the router. Note that this process was not applied to the instruction tokens for the pre-trained large language model. Finally, the projected image feature was concatenated with the filtered instruction token and used as input to the router.

To activate an expert by considering both the given image and instruction, we implemented the router consisting of a single multi-head self-attention block followed by a linear layer. We set the number of translation experts  $K$  engaged in translation to two for all experiments, following previous practices [36, 50]. We pruned experts by applying a threshold to  $E^t$ , removing experts whose corresponding values in  $E^t$  were smaller than  $10^{-3}$ . After identifying redundant experts, we reinitialized those that had not been activated across all tasks learned thus far (i.e., zero-valued entries in the cumulative activation vector  $\mathcal{M}^{1:t}$ ) using the parameters of the visual projector from the pre-trained model.

**Details of the Language Instructions.** The language instructions used as the default setting in our experiments are presented in Table B. For question answering tasks, the instruction varies depending on the sample.

**Measuring Accuracy of Generated Responses.** For the classification and question answering tasks, the performance of the generated responses is evaluated in terms of accuracy. To measure accuracy for classification tasks, we compute the similarity in the embedding space between the textual representations of the classification categories and the generated responses. The predicted class is the category with the highest similarity to the generated response; if it matches the ground truth, the response is considered correct. To compute textual similarity, we extract embeddings using the text encoder of CLIP [40], following [4]. For question answering tasks, the accuracy is determined by whether the answer text appears in the generated response,

Table A. Results on a different task order.

Method	Classification		Captioning		Question Answering	
	Average	$\Delta$ ( $\uparrow$ )	Average	$\Delta$ ( $\uparrow$ )	Average	$\Delta$ ( $\uparrow$ )
<b>Vicuna</b>						
Zero-shot	64.41	0.00	75.00	0.00	51.62	0.00
<b>Last</b>						
LwF [30]	70.78	+6.37	70.46	-4.54	57.18	+5.56
EWC [25]	47.57	-16.84	72.37	-2.63	52.42	+0.80
GMM [4]	60.62	-3.79	73.83	-1.17	54.93	+3.31
EProj [16]	59.26	-5.15	71.41	-3.59	58.97	+7.35
MoEAdapter [50]	66.19	+1.78	75.53	+0.53	47.60	-4.02
MVP (Ours)	<b>86.68</b>	<b>+22.27</b>	<b>77.55</b>	<b>+2.55</b>	<b>70.93</b>	<b>+19.31</b>
<b>Avg</b>						
LwF [30]	62.88	-1.53	65.36	-9.64	52.72	+1.10
EWC [25]	47.43	-16.98	63.03	-11.97	40.43	-11.19
GMM [4]	46.76	-17.65	72.54	-2.46	45.89	-5.73
EProj [16]	47.24	-17.17	72.41	-2.59	45.54	-6.08
MoEAdapter [50]	67.84	+3.43	75.53	+0.53	51.91	+0.29
MVP (Ours)	<b>81.67</b>	<b>+17.26</b>	<b>77.12</b>	<b>+2.12</b>	<b>60.87</b>	<b>+9.25</b>
<b>Transfer</b>						
LwF [30]	70.70	+6.29	63.21	-11.79	49.87	-1.75
EWC [25]	57.77	-6.64	61.92	-13.08	39.85	-11.77
GMM [4]	55.01	-9.40	72.43	-2.57	44.74	-6.88
EProj [16]	50.81	-13.60	72.67	-2.33	43.72	-7.90
MoEAdapter [50]	69.07	+4.66	75.92	+0.92	49.86	-1.76
MVP (Ours)	<b>76.09</b>	<b>+11.68</b>	<b>77.13</b>	<b>+2.13</b>	<b>55.98</b>	<b>+4.36</b>

following previous practices [7, 33].

### B. Additional Experimental Results

**Results on a Different Task Order.** The task order used in Tables 1 and 2 of the main paper follows the sequence of ten classification tasks, four captioning tasks and four question answering tasks. Since captioning and question answering tasks do not have explicit classes, experiments on different class orders are omitted. To evaluate the robustness of the proposed method to a different task order, we conducted additional experiments. We randomly shuffled the task order used in Table 1 of the main paper while keeping all other implementation details the same. Table A reports the experimental results of learning with a random task order. Overall, the proposed method outperforms other continual learning methods. Most competitors show unsatisfactory performance for the three metrics compared to Zero-Shot. Additionally, we report the task-specific performance measured at each time step in Figure A. While other continual learning methods exhibit large performance variations depending on the type of tasks being learned, the proposed method demonstrates robustness with respect to the task order.

**Analysis on Language Instructions.** Additionally, to analyze the robustness of the proposed instruction-grounded

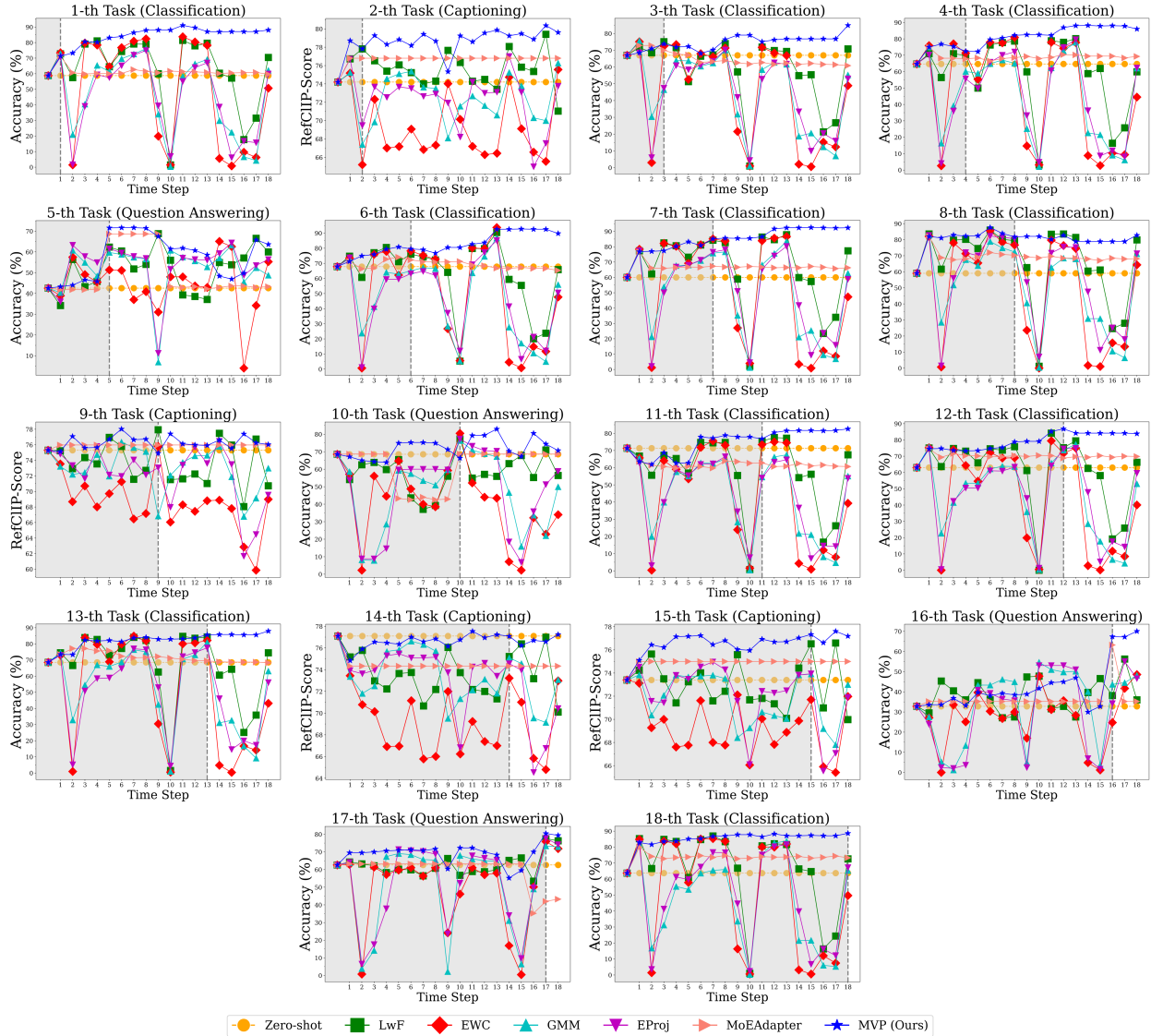


Figure A. Results of training with a random task order, showing the performance of each task at each time step. The yellow horizontal line represents the zero-shot performance of the pre-trained model. The gray area represents the time steps preceding training for specific tasks, and the vertical line indicates the time step at which the corresponding task is learned. Best viewed in color.

visual projector when multiple textual instructions are provided per task, we conducted an additional experiment. We generated ten language instructions using GPT-4o [1] for image classification and captioning tasks. The generated instructions for each task category are shown in the generated response in Table B. For tasks belonging to the corresponding category, one of the ten generated instructions was randomly selected for each sample during training. The experimental results are reported in Table C. The results indicate that the proposed method exhibits robustness, as its performance remains stable regardless of variations in instructions, provided that the instructions maintain contextual consistency. Although an increase in the number

of instructions leads to a slight decline in the transfer performance of the captioning and question answering tasks, the performance measured in *Last* is comparable to those achieved using the default instructions.

**Analysis on Computational Cost.** We analyzed the computational cost of MVP by measuring the wall-clock time and VRAM usage for the experiments in Table 1 of the main paper. The results are summarized in Table D. During its main training phase, MVP requires 20 hours and 48 minutes, a negligible time overhead ( $1.08\times$ ) compared to GMM. This efficiency stems from freezing the computationally expensive vision and language backbones of the VLM while updating only the lightweight components: the

Table B. Language instructions for each type of task.

Task	Classification
Default	· What is this photo of?
Generated	<ul style="list-style-type: none"> <li>· Analyze the image to identify its most detailed category.</li> <li>· The most detailed category should be determined based on the image’s visual features.</li> <li>· Assign the image to the most detailed category by examining its characteristics.</li> <li>· Determine which detailed category best fits the given image and identify it.</li> <li>· Based on the primary subject, identify the detailed category of the image.</li> <li>· The image should be assessed to determine the most detailed category.</li> <li>· Identify the correct detailed category for the given image.</li> <li>· Assign the image to its respective detailed category after carefully identifying its features.</li> <li>· Give the image a detailed category by examining its characteristics.</li> <li>· Given the image’s appearance, identify the appropriate detailed category.</li> </ul>
Task	Captioning
Default	· Describe the given image with a short sentence
Generated	<ul style="list-style-type: none"> <li>· Describe the scene in detail by capturing its key visual elements, interactions, and overall atmosphere.</li> <li>· The scene contains various elements, and it is essential to describe them clearly while maintaining a concise yet informative structure.</li> <li>· Identify and describe the key subjects, their actions, and the interactions that define the scene comprehensively.</li> <li>· A meaningful explanation should effectively describe the scene by considering its composition, significant events, and contextual details.</li> <li>· The scene consists of numerous visual details, so it is important to describe them with clarity to ensure a precise understanding.</li> <li>· Observe the scene carefully and describe the relationships between objects, people, and their interactions within the given context.</li> <li>· Given the scene in the image, provide a well-structured statement that naturally describes its key features and dynamics.</li> <li>· A well-formed caption must thoroughly describe the significant aspects of the scene, ensuring an accurate depiction of its core elements.</li> <li>· As the scene unfolds dynamically, it is necessary to describe its core features with well-structured and concise sentences.</li> <li>· Carefully examine the objects and contextual details in the scene to naturally describe its composition, interactions, and overall atmosphere.</li> </ul>
Task	Question Answering
Default	{Sample-wise Question}
Generated	N/A

Table C. Results using generated instructions.

Method	Classification		Captioning		Question Answering	
	Average	$\Delta$ ( $\uparrow$ )	Average	$\Delta$ ( $\uparrow$ )	Average	$\Delta$ ( $\uparrow$ )
<b>Vicuna</b>						
Zero-shot	64.41	0.00	75.00	0.00	51.62	0.00
<b>Last</b>						
MVP w/ Default	85.87	+21.46	77.75	+2.75	76.34	+24.72
MVP w/ Generated	84.99	+20.58	78.25	+3.25	75.77	+24.15
<b>Avg</b>						
MVP w/ Default	83.28	+18.87	76.94	+1.94	57.68	+6.06
MVP w/ Generated	84.19	+19.78	74.44	-0.56	54.28	+2.66
<b>Transfer</b>						
MVP w/ Default	78.45	+14.04	76.16	+1.16	50.89	-0.73
MVP w/ Generated	79.38	+14.97	72.64	-2.36	45.51	-6.11

router, the set of expert visual projectors, and the learnable pruning vector  $E^t$ . In terms of memory, MVP requires 23.9 GB of VRAM, a marginal increase ( $1.16\times$ ) over GMM from the use of multiple experts. Notably, the subsequent prune and finetune stages are highly efficient, each completing in under 25 minutes and requiring less than 4.0 GB of VRAM. This low cost demonstrates that subsequent learning phase within our framework is highly practical.

**Results on Standard VLM Benchmark.** To measure generalization capability, we evaluated the performance on SEED-Bench [28] after their training on all tasks. As shown in Table E, the compared methods exhibit a significant per-

Table D. Analysis of computational cost.

<b>Vicuna</b>	GMM (train)	EProj (train)	MVP (train / prune / finetune)
Wall-clock time	19h 58min	20h 02min	20h 48min / 24min / 22min
Memory (VRAM)	20.5GB	20.6GB	23.9GB / 4.0GB / 3.1GB

Table E. Results on SEED-Bench after training all tasks.

<b>LLaMa-2</b>	Zero-Shot	GMM	EProj	MoEAdapter	MVP
SEED-Bench [28]	42.66	32.08	29.69	34.72	42.59

formance degradation from the Zero-Shot score, with a performance gap ranging from 7.94 to 12.97. In contrast, MVP achieves a score of 42.59, which is the closest to the Zero-Shot performance. This performance retention is attributed to our adaptive knowledge aggregation strategy. For unseen data, this strategy minimizes the influence of the trained experts and relies on the retained knowledge of the original pre-trained projector, thus preventing performance degradation.